Jurnal Rekayasa Mesin
p-ISSN: 1411-6863, e-ISSN: 2540-7678
Vol.20, No.2, Agustus **2025**, hal. 305-318

Numerical Study of EV Frame Performance in Side Pole Collision: ASTM A36 vs. AL-7075T6 Analysis

Mukhlis Amin*, **Aldias Bahatmaka**
Department of Mechanical Engineering, Universitas Negeri Semarang
Sekaran, Gunungpati, Kota Semarang, 50229
*E-mail: mukhlisaminft@students.unnes.ac.id

Submitted: 19-05-2025; Accepted: 30-08-2025; Published: 31-08-2025

Abstrak

Kendaraan listrik berkembang pesat sebagai alternatif transportasi ramah lingkungan untuk mengurangi emisi gas rumah kaca dan memerangi pemanasan global. Pemerintah Indonesia mendukung transisi ini melalui subsidi, pembangunan infrastruktur, dan regulasi yang mendorong adopsi kendaraan listrik. Produsen otomotif juga berupaya meningkatkan model kendaraan listrik dengan teknologi yang lebih efisien dan aman. Salah satu aspek penting dalam pengembangan kendaraan listrik adalah keselamatan, khususnya ketahanan rangka saat terjadi kecelakaan. Rekayasa struktural berperan besar dalam memastikan keselamatan tersebut, karena kegagalan material akibat beban operasional atau tabrakan dapat menyebabkan kerugian signifikan. Baterai kendaraan listrik yang besar dan berat memberikan tantangan tersendiri dalam merancang rangka yang mampu menopang beban tanpa mengorbankan keselamatan penumpang. Pengujian tabrakan tiang samping menjadi krusial, mengingat ruang penyangga yang terbatas pada sisi kendaraan. Studi ini menganalisis kinerja material ASTM A36 dan AL-7075T6 dalam tabrakan tiang samping pada kecepatan 32 km/jam menggunakan metode *Finite Element Analysis*. Hasil menunjukkan bahwa kedua material mengalami deformasi yang hampir sama, yaitu 98,79 mm untuk ASTM A36 dan 98,77 mm untuk AL-7075T76. Namun, perbedaan signifikan terlihat pada tegangan maksimum, di mana ASTM A36 mencapai 4849,7 MPa, sedangkan AL-7075T6 hanya 1699,9 MPa. Temuan ini menegaskan bahwa AL-7075T6 memiliki ketahanan benturan lebih baik dibandingkan ASTM A36, sehingga berpotensi meningkatkan keselamatan rangka kendaraan listrik dalam kondisi tabrakan tiang samping.

Kata kunci: kendaraan listrik; pengujian tabrak tiang samping; metode elemen hingga; ketahanan terhadap benturan; keamanan struktur

Abstract

Electric vehicles are emerging as eco-friendly alternatives to reduce greenhouse gas emissions and combat global warming. The Indonesian government supports this transition through subsidies, infrastructure development, and regulations encouraging electric vehicle adoption. Automotive manufacturers are enhancing electric vehicle models with safer and more efficient technology. Ensuring the frame's durability during collisions is crucial for safety. Structural engineering plays a vital role, as material failure from operational loads or impacts can lead to significant losses. The large and heavy batteries in electric vehicles present challenges in designing frames that support loads while maintaining passenger safety. Side-pole crash testing is essential due to the limited crumple zones on vehicle sides. This study analyzed the performance of ASTM A36 and AL-7075T6 materials in a side-pole collision at 32 km/h speed using the Finite Element Analysis method. The results showed that both materials experienced almost the same deformation, 98.79 mm for ASTM A26 and 98.77 mm for AL-7075T6. It is, however, a large difference in the maximum stress, ASTM A36 at 4849.7 MPa, and AL-7075T6 at only 1699.9 MPa. This was shown that AL-7075T6 has a better impact resistance than ASTM A36, therefore increasing the safety of electric vehicle frames for side-pole collision conditions.

Keywords: *electric vehicles; side-pole crash test; finite element analysis; crashworthiness; structural safety*

1. Introduction

Electric vehicles (EVs) have been considered environmentally friendly transportation options to reduce greenhouse gas and global warming [1]. In Indonesia, this transformation is significantly propelled by government policies, including purchase subsidies, infrastructure, and regulations that promote the development of the local EV ecosystem [2]. Simultaneously, the automakers have upgraded their EV models with even more efficient and safer technology [3]. In this way, EVs can succeed as a sustainable means of mobility.

With the rapid development of EV technology, safety issues, especially regarding structural safety or vehicle frames in a crash, are now being paid more attention to [4]. Structural engineering is susceptible to problems in the form of material failure due to operational loads, which can lead to losses [5]. The increasing public awareness of transportation safety has driven rapid advancements in navigation and mitigation technologies, aiming to minimize risk during vehicle operations [6]. Moreover, the heavy and large battery pack of EVs imposes structural design challenges, as its frame must be strong enough to bear high loads and should not sacrifice passengers' safety [7]. As a result, EV frames must have adequate strength and ensure the required protection, e.g., of the battery system. Automotive manufacturers continue to develop more substantial frame technologies and materials, as well as protection systems that can reduce the impact of collisions [8]. In addition, various regulations and safety standards are implemented to ensure that electric vehicles have the same or even better safety level than conventional vehicles [9].

A critical aspect of the safety test of electric vehicles is the side-pole crash test, considering that accidents from the side often occur on highways. Side impacts are high risk because the protection area for passengers is more limited due to the lack of sufficient buffer space and energy-absorbing structures, so that the impact force is transmitted directly to the body [10]. In addition, side-pole crashes are no less critical than frontal impacts, as both contribute equally to deaths [11]. Therefore, researchers continue to research to improve a stronger side structure design [12]. The combination of the right materials and reinforced frame design is the main factor in increasing the resistance of electric vehicles to side-pole crashes to provide more optimal protection for passengers.

Recent research highlights the increasing focus on using aluminum alloys in electric vehicle structures, primarily due to their good strength-to-weight ratio and impact energy absorption capabilities. Aluminum-based crash box design reduces the overall vehicle weight and increases the energy absorption capacity, thus strengthening the potential of lightweight materials for structural safety [13]. Despite these advantages, practical barriers such as manufacturing complexity, weldability, and production costs remain important factors in selecting electric vehicle frame materials, especially in emerging markets like Indonesia.

This study uses the Finite Element Analysis (FEA) to study the crashworthiness of two frame materials, ASTM A36 and AL-7075T6, against side-pole impact. In this context, the ASTM A36 and AL-7075T6 are the proposed materials to be used in the comparison analysis, where the ASTM A36 is one of the most common structural steel used in Indonesia because of its availability and low cost, and the AL-7075T6 is one of the lightweight aluminum alloy with high strength-to-weight ratio. Although there are many numerical crashworthiness analysis based on FEA for EV, the number of studies directly comparing these two materials in EV frame safety, especially under side-pole impact, is few. By filling this gap, it is hoped that this research work can provide new knowledge concerning the contribution of the material selection to the structural response that may be useful in forming practical suggestions to enhance the safety and performance of EV frames in Indonesia.

2. Method

2.1. Finite Element Analysis

In this research, the side-pole crash test of an electric vehicle frame is simulated using Finite Element Analysis (FEA) by breaking down complicated structural and mathematical issues into tiny, finite elements connected by nodes [14]. FEA is a numerical method that assesses the mechanical behavior of these elements through computational analysis. By using this method, the impact response, deformation, and stress distribution under crash conditions can all be accurately

predicted. The frame model used in this study was created with SolidWorks CAD software and then imported into ANSYS Explicit Dynamic for crash simulation. The outcomes were then methodically assessed.

2.2. Material

Side-pole crash testing is one of the important tests to analyze vehicle safety during an accident. The electric vehicle frame will hit a stationary pole, with the materials compared in this test simulation being ASTM A36 and AL-7075T6. ASTM A36 material is often used in the automotive and construction industries because of its strong mechanical properties [15]. For comparison, AL-7075T6 material is a material that is equally strong but has a lower density than ASTM A36. The mechanical properties data of ASTM A36 and AL-7075T6 are shown in Table 1.

Table 1. Mechanical Properties of ASTM A36 and AL-7075T6.

No.	Mechanical Properties	ASTM A36	AL-7075T6
1.	Density (g/cm^3)	7.85	2.8
2.	Young's Modulus (GPa)	200	72
3.	Poisson's Ratio	0.26	0.32
4.	Tensile Yield Strength (MPa)	250	480
5.	Ultimate Tensile Strength (MPa)	480	560

2.3. CAD Model Preparation

The EV body structure was developed using SolidWorks CAD software in solid body form to obtain the three-dimensional shape required for crash analysis. A solid formulation was chosen to achieve realistic material thickness, structural continuity, and content interaction during impact. The frame dimensions were extracted based on the average dimensions of the same EV category (e.g., urban compact EV), through standard automotive design methods, to obtain practical aspects and simulation results close to reality. The model has a length of 3491 mm, a width of 1400 mm, and a height of 1331 mm (Figure 1).

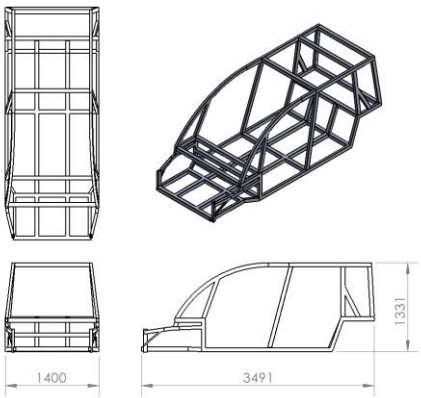

Figure 1. Geometry

2.4. Method Validation

The validation process is carried out to ensure the research is highly accurate and reliable. This validation is done by comparing the simulation results with reference data from previous studies. The main parameter that is validated is stress

in response to impact. With this validation, the method applied in this study can accurately represent the physical phenomena that occur in the crash test scenario.

The validation method in this study involves crash test simulation to evaluate the performance of metal materials in vehicles. Figure 2 shows the geometry taken from the reference article [16]. This approach refers to the same geometry, boundary conditions, and analysis settings described in the reference article. Meanwhile, Table 2 presents the obtained stress values, compared to the reference data and the calculated error rates.

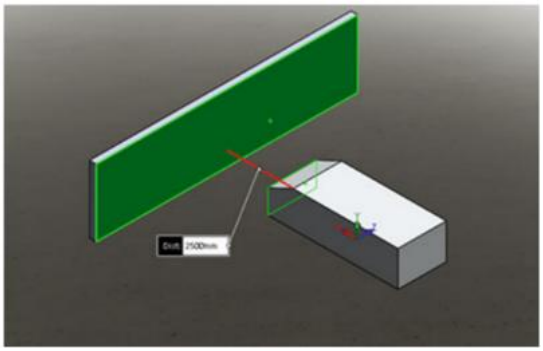

Figure 2. Reference geometry

Table 2. Stress Value vs Reference Stress

Time (s)	Material	Stress (MPa)		Error (%)
		Reference [16]	**Result**	
0.16	Aluminum Alloy	191.15	193	0.97
0.16	Structural Steel	376.04	360.37	4.17

The error obtained in the simulation is less than 5% compared to the reference data. This relatively low error percentage indicates that the deviation between the simulated and actual results is minimal, suggesting a high degree of reliability. Given this level of accuracy, the simulation results can be considered valid and suitable for further analysis. Therefore, these findings provide a strong foundation for subsequent studies, optimizations, or practical applications based on the simulation data.

2.5. Independence Mesh Study

The electric vehicle frame model in this simulation uses a tetrahedron mesh type. Mesh independence analysis is performed to ensure the accuracy of the simulation results. This analysis is an essential step in the simulation where variations in mesh size are applied to ensure that changes in size do not significantly affect the results [17]. Mesh variations start from Mesh A to Mesh E (Table 3). Based on the mesh independence analysis results, Mesh D is selected as the optimal mesh (Figure 3). This selection is based on the stability of the stress values that begin to appear in this mesh compared to other variations that can strengthen the reliability of the simulation results. Figure 4 compares stress values between Mesh A and Mesh E.

Table 3. Independence mesh study.

Mesh Size	Stress (MPa)
Mesh A	230.6

Mesh B	221.53
Mesh C	290.14
Mesh D	308.96
Mesh E	297.99

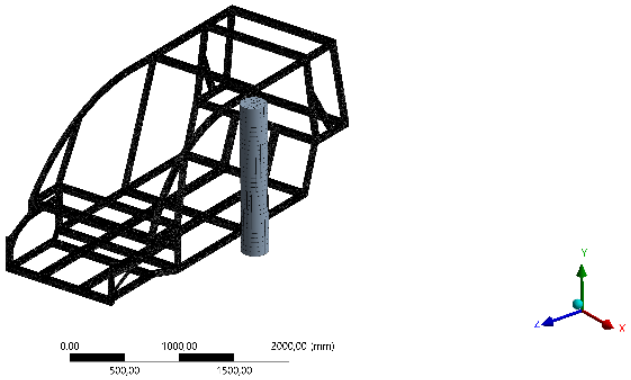

Figure 3. Mesh D

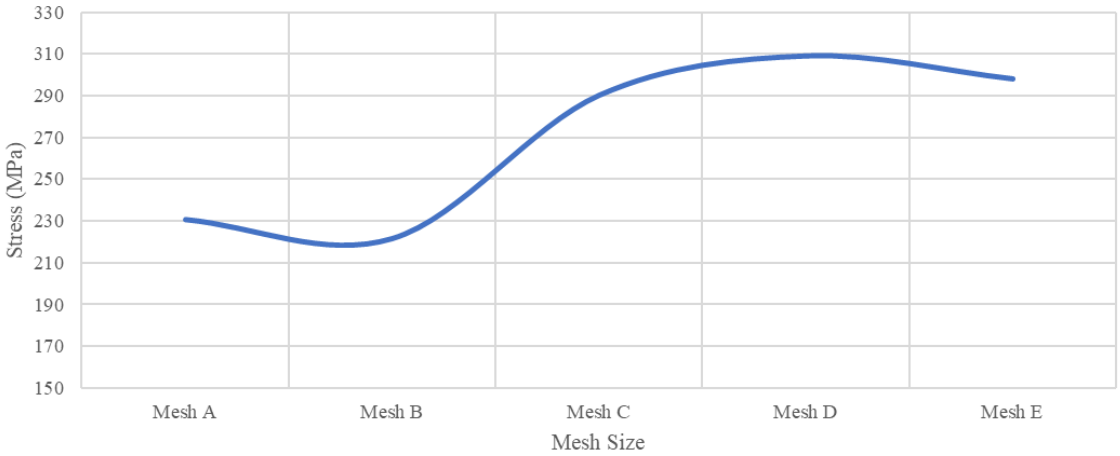

Figure 4. Comparison of stress values between Mesh A and Mesh E

2.6. Boundary Conditions

The next step in the simulation is to establish boundary conditions. In this study, the boundary conditions applied include velocity and fixed support. Determination of these boundary conditions is essential to ensure the accuracy of the simulation results on the response of the frame structure. Fixed support is given at the top and bottom of the pole, at a distance of 0.5 mm from the electric vehicle frame. In contrast, the velocity of the electric vehicle frame is set according to the simulation scenario (Figure 5). The side-pole collision simulation was carried out at 32 km/h speed with the vehicle frame positioned 75° from the pole, a setup that adheres to the side-pole collision rule and is crucial for the accuracy of the simulation [16]. Figure 6 shows the position of the electric vehicle frame about the pole.

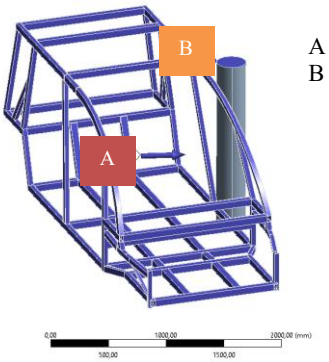

Figure 5. Boundary conditions

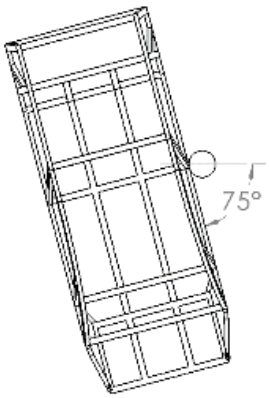

Figure 6. Position of the vehicle

The next step is determining the side-pole collision simulation's end time (s). The end time calculation is given by Equation 1.

$$\text{end time(s)} = \frac{\text{distance(m)}}{\text{speed (m/s}} = \frac{0.0005 \text{ m}}{8.89 \text{ m/s}} = 5.62e^{-5}\text{s} \quad (1)$$

The end time calculation obtained from the equation above is the time required for the electric vehicle frame to reach the pole, so a longer end time is needed to find the maximum stress value under side-pole collision test conditions. This study's end time is $1e^{-2}$ s.

3. Results and Discussion

3.1. Side-Pole Collision Test Simulation

3.1.1. Comparison of ASTM A36 and AL-7075T6 Material Frame Deformation

The side-pole crash test simulation was conducted for $1e^{-2}$ s at an impact velocity of 32 km/h, and the deformation contours of the electric vehicle frame constructed with ASTM A36 and AL-7075T6 materials are presented in Figure 7. At the initial stage, specifically at 0 s (Figure 7(a)), no deformation is observed since the frame has not yet contacted the rigid wall, representing the pre-impact condition. By $3.4e^{-3}$ s (Figure 7(b)), the frame begins to undergo visible deformation, with maximum values of 31.807 mm for ASTM A36 and 31.867 mm for AL-7075T6, indicating that both materials initially respond in a nearly identical manner under the applied load. As the impact progresses to $6.65e^{-3}$ s (Figure 7(c)), deformation intensifies, reaching 62.919 mm for ASTM A36 and 62.959 mm for AL-7075T6. This suggests

that energy absorption during mid-impact is distributed relatively evenly between the two materials. Finally, at the end of the simulation ($1e^{-2}$ s (Figure 7(d)), the maximum deformation reaches 98.79 mm for ASTM A36 and 98.774 mm for AL-7075T6. The close agreement between these values implies that both materials exhibit a similar capacity to undergo plastic deformation under side-pole collision loading. The progressive increase in deformation over time illustrates the expected crashworthiness behavior of the frame, where structural displacement grows in proportion to the impact duration and energy transfer. A detailed summary of the deformation values at each time step is provided in Table 4. Figure 8 highlights the minimal difference in deformation trends between ASTM A36 and AL-7075T6.

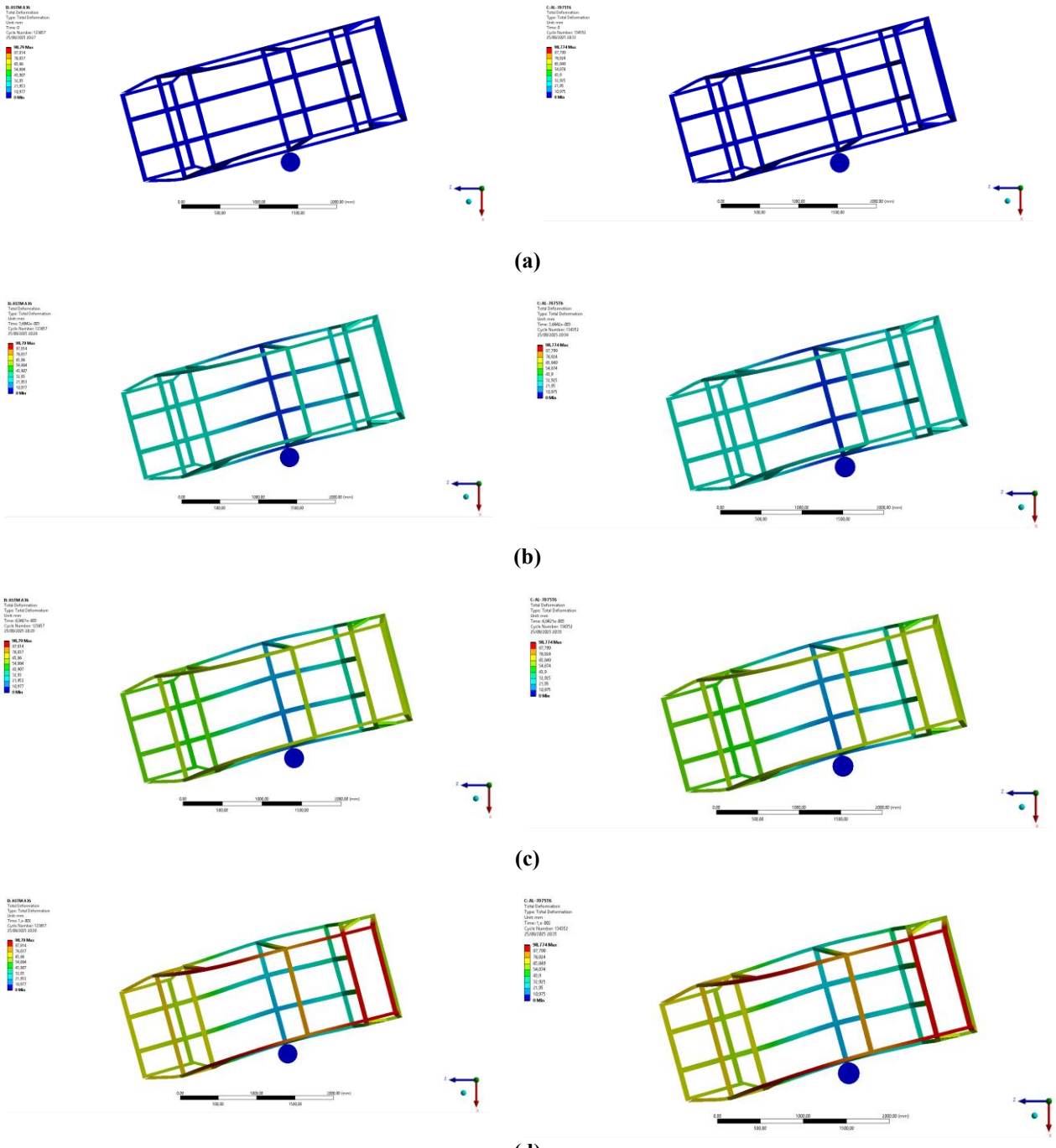

Figure 7. ASTM A36 (left) and AL-7075T6 (right) vehicle frame deformation: (a) 0 s; (b) $3.4e^{-3}$ s; (c) $6.65e^{-3}$ s; (d) $1e^{-2}$ s

Table 4. Deformation vs Time

Time (s)	Deformation (mm)	
	ASTM A36	AL-7075T6
0	0	0
$3.4e^{-3}$	31.807	31.867
$6.65e^{-3}$	62.919	62.959
$1e^{-2}$	98.79	98.774

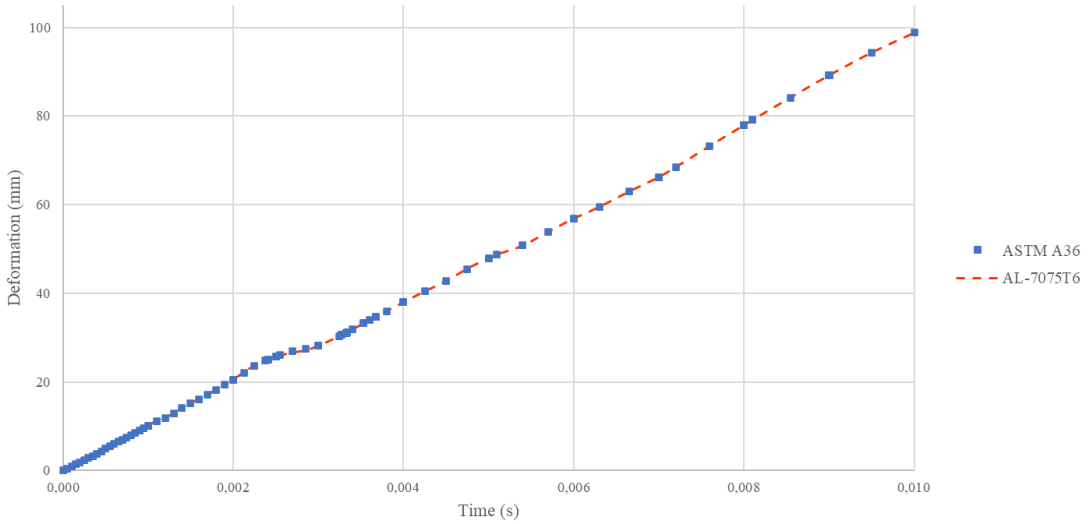

Figure 8. Comparison of deformation values of ASTM A36 and AL-7075T6 frames

Based on the data shown in Figure 8, it can be observed that the overall deformation of both materials appears nearly identical despite their different mechanical properties. Scientifically, this can be explained by the fact that under identical frame geometry, thickness, and impact load conditions, the deformation response is more influenced by the load distribution path and global failure mode of the structure, rather than solely by the material properties [18]. Steel, with its higher elastic modulus but lower yield strength, tends to enter the plastic region more quickly, while high-strength aluminum alloys can withstand higher stress while remaining elastic for a longer duration [19]. As a result, the final deformation obtained in this study is relatively similar, which is consistent with previous crashworthiness simulations involving both steel and aluminum alloys [19].

3.1.2. Comparison of ASTM A36 and AL-7075T6 Material Frame Stress

The side-pole crash test simulation was carried out for a duration of $1e^{-2}$ s at a 32 km/h velocity. The temporal evolution of stress development during the collision is depicted in Figure 9, which presents the stress contour distributions of ASTM A36 and AL-7075T6 at several times. As illustrated in Figure 9(a), at the initial stage, no stress was recorded because the vehicle frame had not yet contacted the rigid wall. Therefore, no deformation had taken place. Once contact occurred, as shown in Figure 9(b) at $3.4e^{-3}$ s, stress began to distribute across the frame, with the maximum values recorded as 2436.2 MPa for ASTM A36 and 874.46 MPa for AL-7075T6. These results indicate that although both materials were subjected to identical loading conditions, the steel frame exhibited a higher peak stress level due to its different yield characteristics and elastic-plastic behavior than the aluminum alloy.

The progression of stress with increasing simulation time is further demonstrated in Figure 9(c), corresponding to $6.65e^{-3}$ s. At this stage, the maximum stress values were measured at 2917.7 MPa for ASTM A36 and 1053.5 MPa for AL-7075T6. With a further time increment, corresponding to Figure 9(d), the maximum stress values increased significantly, reaching 3132.5 MPa for ASTM A36 and 1140.1MPa for AL-7075T6. This increase highlights the progressive accumulation of stress within the frame as deformation propagated through the structure, indicating that the materials continued to absorb and distribute the impact energy throughout the simulation. A detailed summary of these results is presented in Table 5.

Figure 10 illustrates the location of the maximum stress for both ASTM A36 and AL-7075T6 materials during the crash simulation. It can be clearly observed that the highest stress occurs at the same structural region for both materials, indicating that the geometry of the frame plays a dominant role in determining the stress concentration zone. This similarity suggests that stress distribution is more strongly influenced by the overall structural design and load transfer path under identical loading and boundary conditions, rather than the type of material alone. Such findings reinforce the idea that, while the magnitude of stress differs significantly between steel and aluminum alloys, the critical regions of failure initiation remain consistent across different materials due to identical frame geometry.

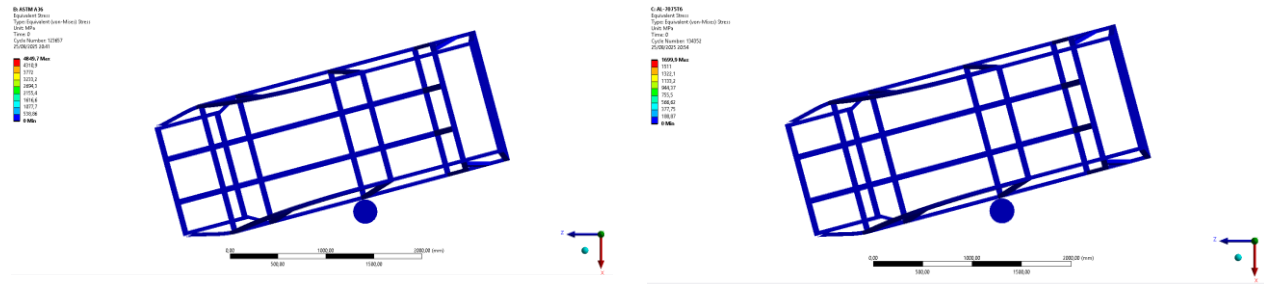

(a)

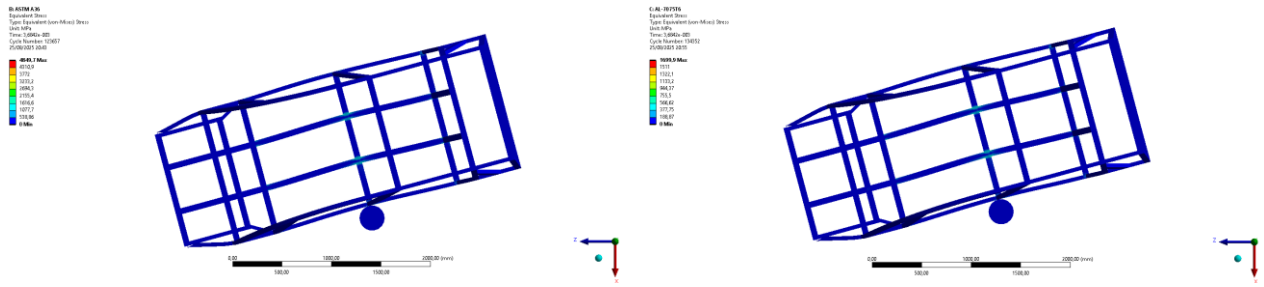

(b)

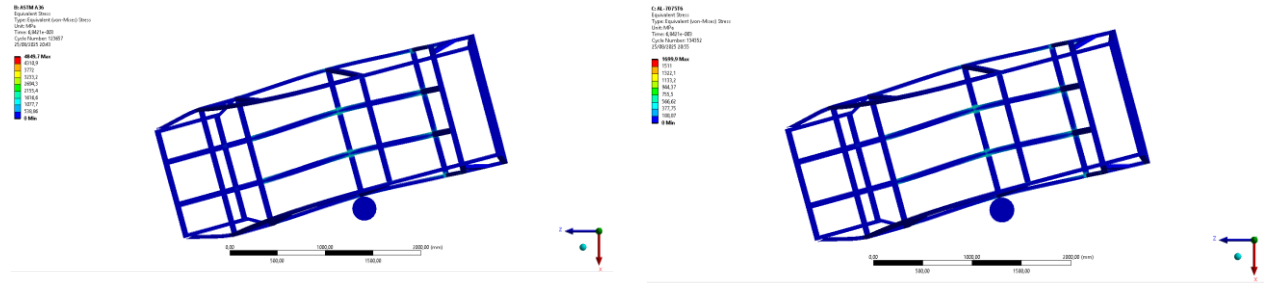

(c)

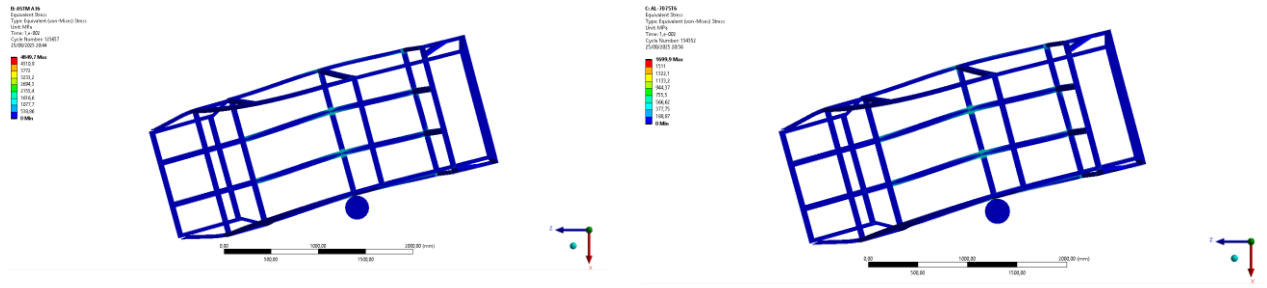

(d)

Figure 9. ASTM A36 (left) and A:-7075T6 (right) vehicle frame stress: (a) 0 s; (b) $3.4e^{-3}$ s; (c) $6.65e^{-3}$ s; (d) $1e^{-2}$ s

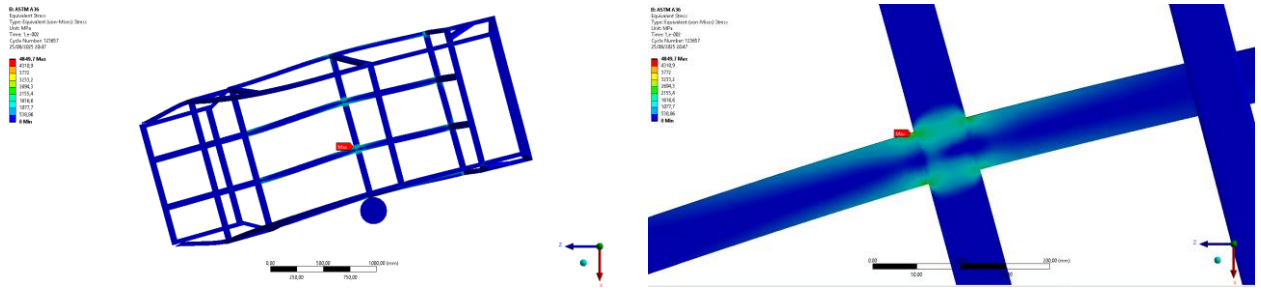

(a)

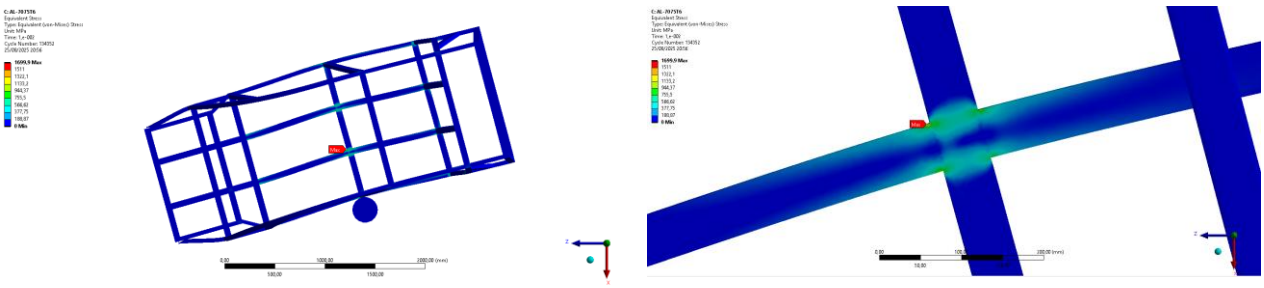

(b)

Figure 10. Highest stress point: **(a)** ASTM A36; **(b)** AL-7075T6

Table 5. Stress vs Time

Time (s)	Stress (MPa)	
	ASTM A36	AL-7075T6
0	0	0
$3.4e^{-3}$	2436.2	874.46
$6.65e^{-3}$	2917.7	1053.5
$1e^{-2}$	3132.5	1140.1

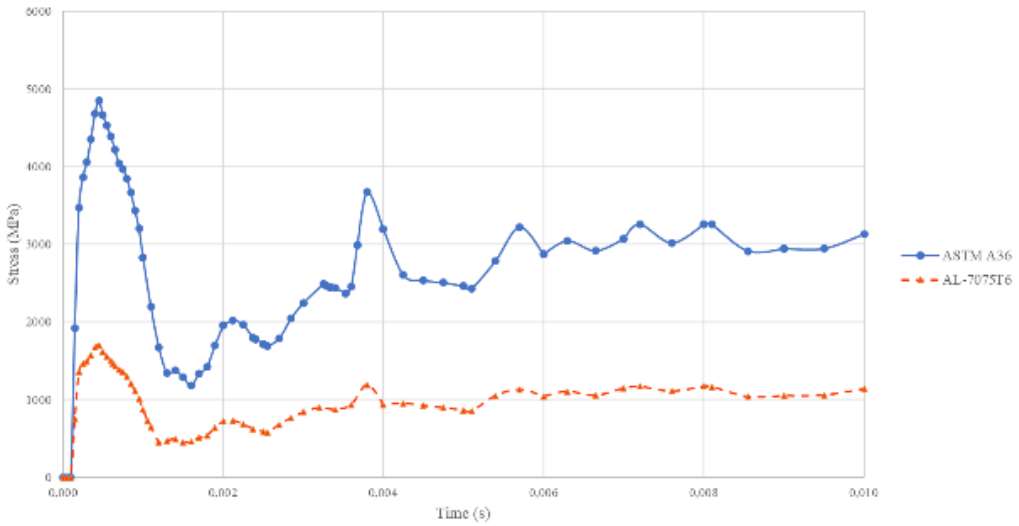

Figure 11. Comparison of stress values of ASTM A36 and AL-7075T6 frames

Figure 11 compares the stress between ASTM A36 and AL-7075T6 materials under a side-pole impact. In the initial impact stage, ASTM A36 recorded a sharp stress spike, reaching its maximum value of 4849.7 MPa at $4.5e^{-4}$ s, while AL-7075T6 reached a much lower peak of 1699.9 MPa at the same time. After this initial peak, the stress response of both materials decreased but followed different patterns: ASTM A36 showed clear fluctuations throughout the simulation, reflecting unstable stress redistribution and recurring concentration zones as deformation progressed, while AL-7075T6 showed a smoother and more stable reduction with only slight variations, indicating its ability to dissipate impact energy more uniformly.

3.1.3. Comparison of ASTM A36 and AL-7075T6 Material Frame Safety Factor

The side-pole crash test was simulated for a duration of $1e^{-2}$ s at an impact velocity of 32 km/h, and the resulting safety factor contours of the electric vehicle frame using ASTM A36 and AL-7076T6 materials are presented in Figure 12. However, once the frame collides with the rigid barrier, apparent variations in the safety factor between the two materials emerge. Specifically, the frame constructed from AL-7075T6 consistently demonstrates a higher safety factor than that of ASTM A36, indicating that AL-7075T6 can resist critical stress concentrations during impact.

The higher safety factor values observed in the AL-7075T6 frame imply that this material can tolerate larger applied stresses relative to its strength limit before failure occurs, reducing the likelihood of localized plastic collapse or catastrophic fracture. In contrast, ASTM A36 exhibits lower safety factor values, suggesting a reduced margin of safety under the same loading conditions. This distinction highlights the superior structural integrity and durability of AL-7075T6, which can be attributed to its strength-to-weight ratio than conventional steels.

From a crashworthiness perspective, the implications of these findings are significant. A higher safety factor improves the frame's ability to withstand deformation and enhances occupant protection by minimizing excessive intrusion into the passenger compartment during a side-pole collision. Consequently, the use of AL-7075T6 in vehicle frame design offers clear advantages in improving structural resilience, ensuring better energy absorption, and ultimately increasing the vehicle's overall safety performance. These results further reinforce the suitability of lightweight aluminum alloys, particularly AL-7075T6, in modern electric vehicle applications where safety and weight reduction are essential design objectives.

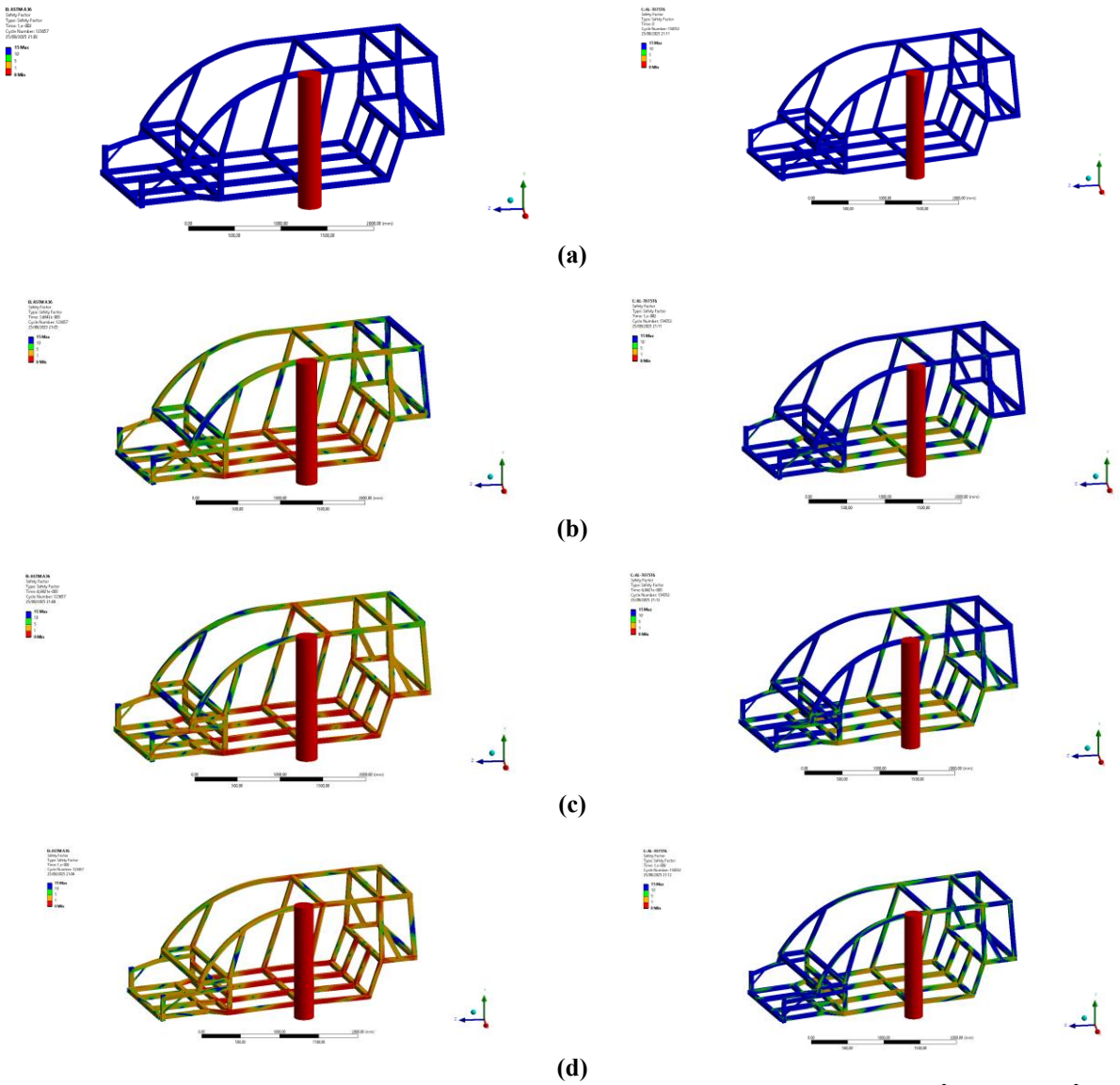

Figure 12. ASTM A36 (left) and A:-7075T6 (right) vehicle frame safety factor: (a) 0 s; (b) $3.4e^{-3}$ s; (c) $6.65e^{-3}$ s; (d) $1e^{-2}$ s.

4. Conclusion

This study presented the design and crashworthiness evaluation of an electric vehicle frame using two materials, ASTM A36 and AL-7075T6, under a side-pole collision scenario at 32 km/h and 75° impact angle. The simulation results indicate that both materials exhibit nearly identical deformation values, suggesting that material substitution minimally influences overall displacement response. This similarity in deformation can be attributed to the geometric configuration of the frame and the boundary conditions of the crash test, where the overall structural stiffness dominates the response, resulting in comparable displacement behavior regardless of the material used.

However, significant differences are observed in stress distribution and safety factor. ASTM A36 generates higher peak stress values (4849.7 MPa) than AL-7075T6 (1699.9 MPa), although the stress remains localized at specific frame regions. In contrast, the AL-7075T6 frame demonstrates higher safety factor values, reflecting superior structural resistance and improved crashworthiness performance.

Overall, these findings highlight the potential of AL-7075T6 as a lightweight alternative to conventional steel for electric vehicle frames, combining reduced weight with enhanced safety margins. Future research should focus on the structural design optimization, particularly at sharp angles and joints where stress concentrations are most severe, to

minimize deformation and improve energy absorption characteristics. Such improvements are essential to enhance passenger protection and ensure compliance with advanced vehicle safety standards.

Acknowledgement

Through this statement, the author would like to express his gratitude to the Department of Mechanical Engineering Universitas Negeri Semarang, which has helped the author complete the research.

References

[1] R. Hidayat and J. Cowie, "A framework to explore policy to support the adoption of electric vehicles in developing nations: A case study of Indonesia," *Transp. Res. Procedia*, vol. 70, pp. 364–371, 2023, doi: 10.1016/j.trpro.2023.11.041.

[2] N. C. Kresnanto and W. H. Putri, "Subsidies for electric vehicles as a form of green transportation: Evidence from Indonesia," *Transp. Res. Interdiscip. Perspect.*, vol. 27, February, p. 101230, 2024, doi: 10.1016/j.trip.2024.101230.

[3] R. T. Yadlapalli, A. Kotapati, R. Kandipati, and C. S. Koritala, "A review on energy efficient technologies for electric vehicle applications," *J. Energy Storage*, vol. 50, no. January, p. 104212, 2022, doi: 10.1016/j.est.2022.104212.

[4] U. Idrees *et al.*, "Finite element analysis of car frame frontal crash using lightweight materials," *J. Eng. Res.*, vol. 11, no. 1, 2023, doi: 10.1016/j.jer.2023.100007.

[5] A. Fajri, A. R. Prabowo, N. Muhayat, D. F. Smaradhana, and A. Bahatmaka, "Fatigue analysis of engineering structures: State of development and achievement," *Procedia Struct. Integr.*, vol. 33, no. C, pp. 19–26, 2021, doi: 10.1016/j.prostr.2021.10.004.

[6] A. R. Prabowo, A. Bahatmaka, and J. M. Sohn, "Crashworthiness characteristic of longitudinal deck structures against identified accidental action in marine environment: a study case of ship–bow collision," *J. Brazilian Soc. Mech. Sci. Eng.*, vol. 42, no. 11, pp. 1–13, 2020, doi: 10.1007/s40430-020-02662-2.

[7] E. Cebe, O. Kalbaran, and A. B. Irez, "A numerical investigation of ground impact for hierarchically designed hybrid composite structures in electric vehicle battery cases," *J. Power Sources*, vol. 638, no. December 2024, p. 236594, 2025, doi: 10.1016/j.jpowsour.2025.236594.

[8] X. Zhu, W. Wang, W. Li, Q. Zhang, G. Lei, and Q. X. Wu, "Impact resistance of bridge columns with energy-absorbing crash dampers under vehicle collisions," *J. Constr. Steel Res.*, vol. 218, no. April, p. 108740, 2024, doi: 10.1016/j.jcsr.2024.108740.

[9] A. B. Navale, S. P. Chippa, D. A. Chougule, and P. M. Raut, "Crashworthiness aspects of electric vehicle design," *Int. J. Crashworthiness*, vol. 26, no. 4, pp. 368–387, 2021, doi: 10.1080/13588265.2020.1718462.

[10] R. Yang, S. Li, T. Cheng, P. Zou, and L. Tian, "Enhanced Side Pole Impact Protection: Crashworthiness Optimization for Electric Micro Commercial Vehicles," *Appl. Sci.*, vol. 15, no. 4, 2025, doi: 10.3390/app15042220.

[11] A. Gashu and R. B. Nallamothu, "Improvement of crashworthiness of pickup vehicle for frontal and side collision using Finite Element analysis," *Adv. Mech. Eng.*, vol. 17, no. 2, pp. 1–16, 2025, doi: 10.1177/16878132251322029.

[12] Z. Hongxue, W. Sanxia, L. Xiao, P. Zhifei, and Z. Guosheng, "Optimization for Side Structure of Vehicle Based

on FEA," *Procedia Comput. Sci.*, vol. 208, pp. 196–205, 2022, doi: 10.1016/j.procs.2022.10.029.

[13] S. Malaimeham and S. Vinaitheerthan, "Performance improvement of steel and aluminum crush box with mass optimization by using finite element method," *Rev. Mater.*, vol. 29, no. 4, 2024, doi: 10.1590/1517-7076-RMAT-2024-0568.

[14] A. Verma *et al.*, "Finite element analysis and its application in Orthopaedics: A narrative review," *J. Clin. Orthop. Trauma*, vol. 58, no. November, p. 102803, 2024, doi: 10.1016/j.jcot.2024.102803.

[15] R. P. Putra *et al.*, "Design and Crash Test on a Two-Passenger City Car Frame using the Finite Element Method," *Automot. Exp.*, vol. 7, no. 2, pp. 270–283, 2024, doi: 10.31603/ae.11306.

[16] C. M. Choudhari, J. Desai, S. Bhavsar, and D. Choudhary, *Crash simulation of an Automotive Body to Explore Performance of Different Metallic Materials using ANSYS*. Springer Singapore, 2019. doi: 10.1007/978-981-13-2490-1_64.

[17] T. Oktay and Y. Eraslan, "Mesh Independence Study On Computational Fluid Dynamics (CFD) Analysis of A Quad-Rotor Uav Propeller," *3 . Int. Eur. Conf. Interdiscip. Sci. Res.*, no. 1, 2021.

[18] M. Alardhi, R. Sequeira, M. Fahed, J. Alrajhi, and K. Alkhulaifi, "applied sciences Assessing the Crashworthiness Analysis on Frontal and Corner Impacts of Vehicle on Street Poles Using FEA," 2022.

[19] P. Kaczynski, "Crashworthiness Characteristic of Dynamically Expanded Circular Tubes Made of Light Alloys :," 2020, doi: 10.3390/ma13235332.